Journal of Inclusion Phenomena and Molecular Recognition in Chemistry **8**: 3–16, 1990.

Dielectric and ^{13}C NMR Studies of the Carbon Monoxide Clathrate Hydrate*

M. A. DESANDO, Y. P. HANDA, R. E. HAWKINS, C. I. RATCLIFFE**, and J. A. RIPMEESTER
Division of Chemistry, National Research Council of Canada, Ottawa, Ontario, Canada K1A 0R9

(Received: 28 March 1988; in final form: 4 May 1988)

Abstract. The structure I clathrate hydrate of carbon monoxide has been studied using dielectric measurements and ^{13}C NMR spectroscopy. Broad, weak dielectric absorption curves with maxima at 2.2–3.8 K yield $E_a = 0.14$ kJ mol^{-1} for the average Arrhenius activation energy associated with the reorientation of the low polarity guest. Except for H_2S this represents the fastest reorienting polar guest known among the clathrate hydrates. The low temperature dielectric absorption curves can best be fitted with a Cole–Davidson asymmetric distribution of relaxation times and activation energies (with $\theta = 0.06$ at 4×10^6 Hz), which at 10^7 Hz has been resolved into a double symmetric distribution of discrete relaxation times for CO in the small and large cages. The cross-polarization magic angle spinning ^{13}C NMR spectra indicate identical chemical shifts for CO in the small and large cages, in contrast to other hydrates. The static spectra show that the CO molecules undergo anisotropic reorientation in the large cages and that there is still considerable mobility at 77 K. One possible model for the anisotropic motion has the CO rapidly moving among sites over each of the 14 faces of the cage with the CO axis orientated towards the cage centre. The cage occupancy ratio at 220 K, $\theta_S/\theta_L = 1.11$, indicates slightly greater preference of CO for the small cage.

Key words. Carbon monoxide hydrate, dielectrics, ^{13}C NMR, molecular motion.

1. Introduction

In a recent note we reported the preparation and characterization of the clathrate hydrate of carbon monoxide [1]. X-ray diffraction in conjunction with dielectric and ^{13}C NMR results firmly established that the CO hydrate forms a structure I cubic hydrate. This is in marked contrast to other very small but non-polar guest molecules which form structure II cubic hydrates [2–5], including O_2 and N_2 which are of similar size to CO.

Structure I and II clathrate hydrates both consist of a host lattice of hydrogen bonded water molecules which form cages around the guest molecules [43, 46]. The structure I unit cell contains 46 H_2O molecules forming 2 12-hedral cages and 6 14-hedral cages, whereas the structure II unit cell contains 136 H_2O molecules forming 16 12-hedral cages and 8 16-hedral cages. There is therefore a greater ratio of small to large cages in structure II. The small cages of structure I and the large cages of structure II have cubic symmetry and are thus virtually spherical cavities,

Published as NRCC No. 30428.
* Dedicated to Dr D. W. Davidson in honor of his great contributions to the sciences of inclusion phenomena.
** Author for correspondence.

whereas the small cages of structure II and in particular the large cages of structure I are not spherical.

Bar-Nun *et al.* [6] have probably produced CO hydrate in the laboratory on a previous occasion, while studying the trapping and release of gases by ice under conditions similar to those experienced in space. CO hydrate is thought to be a constituent of cometary nuclei and may be present on the satellites of the outer planets [6–14].

In this paper we present a more detailed analysis of our dielectric and ^{13}C NMR studies of CO hydrate, with particular emphasis on the dynamics of the CO molecules and their occupancy of the small and large cages. The dipole moment and the direction of the principal axis of the unique component of the ^{13}C chemical shift tensor must be coincident with the CO bond axis. Thus the dielectric and ^{13}C NMR studies can provide information which relates directly to the reorientation of the bond. Furthermore, previous NMR studies of other structure I hydrates [15–17] have clearly shown that guest molecules possessing a unique axis undergo anisotropic motion in the large 14-hedral cage, which has a roughly oblate spheroidal shape. On account of the small size of CO one would expect considerably more reorientational freedom and a much higher occupancy of the small 12-hedral cages than for larger guest molecules.

2. Experimental

The preparation of the samples has been described previously [1]. The sample for the ^{13}C NMR study was prepared from gas enriched to 50% in ^{13}CO (from MSD Isotopes Ltd.).

For the dielectric experiments samples of the hydrate were pressed at about 1.1 kbar, in a die immersed in liquid nitrogen, into the form of 1.905 cm diameter discs. Dielectric measurements were made at frequencies in the range 10^3–5×10^4 Hz on a General Radio 1615-A capacitance bridge, and in the range 10^3–10^7 Hz on a Hewlett-Packard 4275A Multi-Frequency LCR meter, and at temperatures between 1.7–150 K. Frequencies of the applied electric field across the sample were checked during the course of the measurements on a Hewlett-Packard 5223L electronic counter, and with the timebase of a Tektronix type 564B storage oscilloscope. Other details of the apparatus and cryogenic system have been given previously [18].

^{13}C NMR spectra were obtained at 45.3 MHz on a Bruker CXP-180 pulse spectrometer. ^1H–^{13}C cross-polarization (CP) spectra were obtained with a CP time of 5 ms [19]. Bloch decay spectra (no CP) were obtained using phase cycling. Magic angle spinning (MAS) CP spectra were obtained using a Chemagnetics variable temperature probe. The sample was packed into a Delrin spinner at liquid nitrogen temperatures and the spinner was then loaded into the pre-cooled probe. The temperature was maintained in the range 143–153 K throughout the MAS experiment and the spinning rate was 2.2 kHz. Spectra of the static sample were obtained at 77 K and above using a modified Bruker CP probe. The sample for the latter experiment was sealed into a thick-walled small-diameter glass tube, in order to allow measurements at temperatures as high as 220 K, where considerable pressure build-up occurs, due to dissociation of the hydrate. High-power proton decoupling was used during the data acquisition period for all the spectra.

3. Results and Discussion

3.1. DIELECTRIC MEASUREMENTS

Example plots of the dielectric loss factor ϵ'' versus temperature T (or $1/T$) are shown in Figures 1–3. Two regions of dielectric absorption occur: (i) above ~ 150 K, from the relaxation of the host water molecules; and (ii) below ~ 30 K, from carbon monoxide in the clathrate cages. The latter absorption is very much weaker because of the small dipole moment of CO (about 0.13 Debye in the gas phase [20]). Relevant data are given in Table I. Here we shall be concerned principally with the CO relaxation.

The reciprocal temperature dependence of ϵ'' suggests that there is a wide distribution of relaxation times and activation barriers for dipole orientation [21] for which there is ample evidence from other dielectric and NMR studies of clathrate hydrates [22]. A relaxation process characterized by a single time constant for the exponential decay of the orientation polarization would exhibit much narrower and symmetric absorption curves ($\beta = 1$) (Figure 2). The distributions arise as a result of the frozen-in orientational disorder of the host water molecules which produces a distribution of slightly different cages.

In order to gain further information on the nature of the clathrate dielectric absorption, calculations were made of the loss factor from different distribution models. Both symmetric (Cole–Cole [23]; Equation (1), Fuoss–Kirkwood [24]; Equation (2)) and asymmetric (Cole–Davidson [25]; Equation (3)) functions were employed in the analyses. In Equations (1)–(3)

$$\epsilon'' = \frac{\Delta\epsilon \cos(\alpha\pi/2)}{2\{\cosh((1-\alpha)\ln \omega t) + \sin(\alpha\pi/2)\}}; \qquad 0 \leqslant \alpha < 1 \tag{1}$$

$$\epsilon'' = \epsilon''_{\max}\{\cosh(\beta \ln \omega t)\}^{-1}; \qquad 0 < \beta \leqslant 1 \tag{2}$$

$$\epsilon'' = \Delta\epsilon\{\cos^{\theta}[\arctan(\omega t)]\} \sin[\theta \arctan(\omega t)]; \qquad 0 < \theta \leqslant 1 \tag{3}$$

Table I. Apparent dielectric absorption and dispersion data of carbon monoxide clathrate hydrate at low temperatures.

	Frequency (Hz)			
	4×10^5	10^6	4×10^6	10^7
[a] $T_{\max}$	2.2 ± 0.3	2.6 ± 0.2	3.3 ± 0.3	3.8 ± 0.4
[b] $\epsilon''_{\max}$	0.112	0.0123	0.0164	0.0310
[c] Δe	–	$\gtrsim 0.035$	$\gtrsim 0.034$	$\gtrsim 0.050$
[d] μ(Debye)	0.08	0.09	0.09	0.10

[a] Temperature of maximum dielectric loss factor (See Ref. [1] for dielectric absorption curves at 4×10^5 and 10^6 Hz).
[b] At 10^7 Hz residual inductance from the leads and electrode may contribute appreciably to the error on the value of ϵ''.
[c] Low limit values owing to the fact that the dielectric dispersion is not complete at 1.7 K.
[d] From the slope of the ϵ' versus $1/T$ plots.

$\Delta\epsilon = \epsilon_0 - \epsilon_\infty$, is the difference between the low and high frequency limits of the relative dielectric permittivity, i.e. the amplitude of the dielectric dispersion, and α, β, and θ are the distribution parameters which tend to $\alpha = 1$, $\beta = 0$, and $\theta = 1$ as the Debye limit for a single relaxation time is approached. The latter condition also specifies that the maximum loss factor is $\epsilon''_{max} = \Delta\epsilon/2$. At a certain temperature the relaxation time (τ) is determined by the activation barrier (E_a) and the pre-exponential factor (τ_0): $\tau = \tau_0 \exp(E_a/RT)$.

A plot of the logarithm of the frequency at which the maximum dielectric loss occurs versus reciprocal temperature should be linear and the Arrhenius activation energy can be obtained from the slope. In the present case the uncertainty in the peak position, owing to the width and asymmetry of the dielectric absorption, leads to an *average* activation barrier of 0.14 kJ mol^{-1} between the limiting values of 0.09 and 0.54 kJ mol^{-1}. This barrier compares with an estimate of $\leqslant$0.210 kJ mol^{-1} for hydrogen sulfide clathrate hydrate whose dielectric loss maxima have not been observed, but lie below 2 K at 1 MHz [22]. The activation energy for carbon monoxide in the clathrate hydrate is also appreciably less than those for CO–N_2–Ar quadrupole glasses [26] (e.g., $E_a = 0.906$ kJ mol^{-1} for $CO_{0.10}N_{2(0.20)}Ar_{0.70}$ and 1.92 kJ mol^{-1} for $CO_{0.30}N_{2(0.30)}Ar_{0.40}$), solid α-phase CO [27] ($E_a = 6.13$ kJ mol^{-1}) and CO–β-quinol clathrate [28] ($E_a = 4.6$ kJ mol^{-1}). There is, however, uncertainty as to the exact nature of the relaxation process in the glass and pure solid.

Trial values of α, τ_0, and E_a were used to generate the curve of best fit to the experimental loss data. It was found that the dielectric absorption at 4×10^6 Hz is best described by a Cole–Davidson distribution model, with $\theta = 0.06$ (Figure 2). This suggests a changing distribution of relaxation times, and more than one

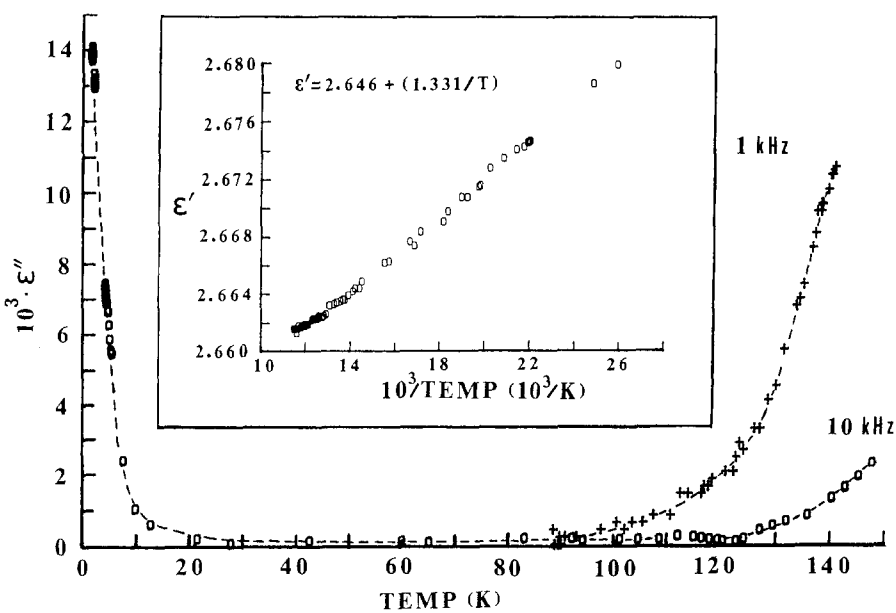

Fig. 1. Low and high temperature dielectric absorptions of the carbon monoxide clathrate hydrate.

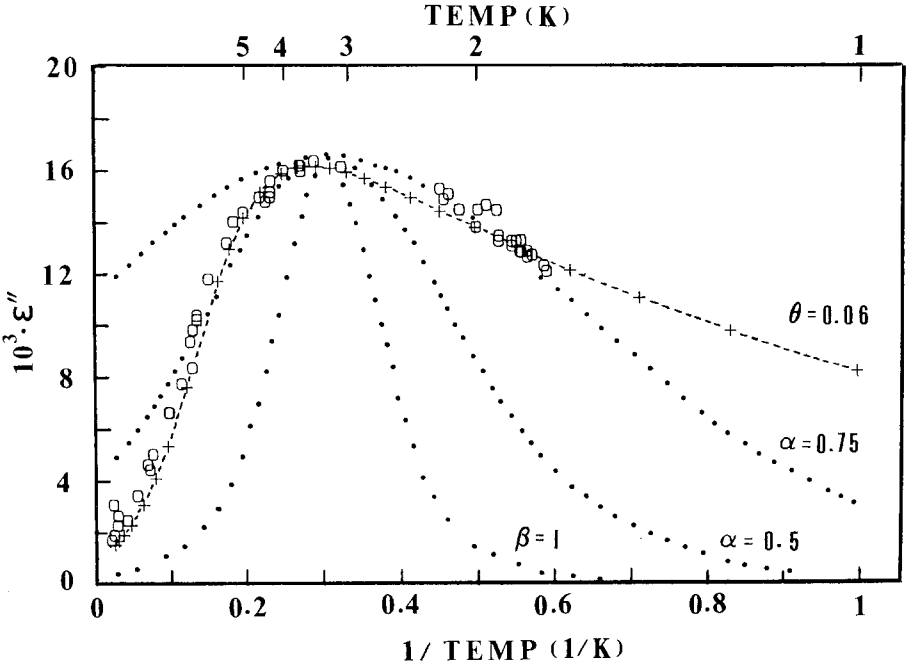

Fig. 2. Observed (○) and calculated low temperature dielectric absorption at 4×10^6 Hz of carbon monoxide clathrate hydrate. (+, $\Delta\epsilon = 0.2137$, $\tau_0 = 3.5 \times 10^{-9}$ s), ($\alpha = 0.75$, $\Delta\epsilon = 0.165$, $\tau_0 = 2.11 \times 10^{-10}$ s), ($\alpha = 0.5$, $\Delta\epsilon = 0.080$, $\tau_0 = 2.11 \times 10^{-10}$ s), ($\beta = 1$, $\Delta\epsilon = 0.033$, $\tau_0 = 2.11 \times 10^{-10}$ s); ($E_a = 0.14$ kJ mol^{-1}).

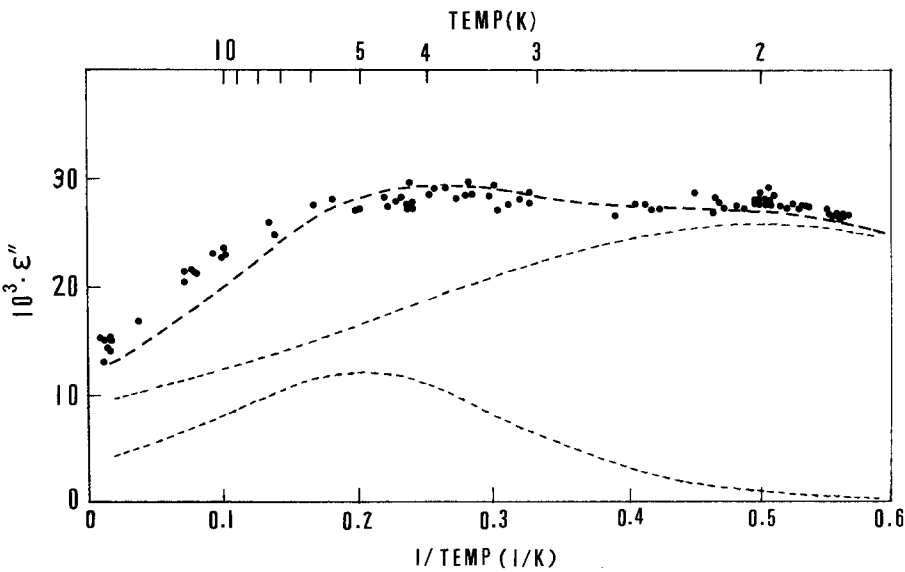

Fig. 3. Observed (·) and calculated (– – –) low temperature dielectric absorption at 10^7 Hz of carbon monoxide clathrate hydrate. The top curve is the sum of the two component absorption curves.

independent relaxation process. Furthermore, the asymmetry of the peaks is consistent with a distribution of energy barriers. A skewing of the dielectric absorption towards low temperatures has been observed for other clathrate hydrates, *viz.*, dimethyl ether and tetrahydrofuran [29, 30]. A Budó [31, 32] type of analysis in terms of a weighted amplitude of dielectric dispersion was therefore applied to the 10^7 Hz CO hydrate data (Figure 3). In Equation (4) C is the weighting factor

$$\epsilon'' = \sum_i \left(\frac{C_i \, \Delta\epsilon\omega\tau_i}{1 + \omega^2\tau_i^2} \right); \qquad \sum C_i = 1 \tag{4}$$

which reflects the contribution of each discrete relaxation process to the overall dielectric absorption. The C value also has a dependence on the concentration (X) of relaxing dipole moment components (μ):

$$C = X_i\mu_i^2 \Big/ \sum_i X_i\mu_i^2. \tag{5}$$

In the case of structure I CO hydrate the limiting ratio of the number of guest molecules in the 12- and 14-hedral cages is expected to be close to 1 : 3 (A ratio of 1 : 2.7 is in fact obtained from the analysis of the ^{13}C NMR results at 220 K, though some decomposition was evident at this temperature (see below)). Consequently, if the same dipole moment component, e.g. along the C—O axis, is involved in the relaxation in both types of cages, then $C_S/C_L = 1/3$. Evidence which suggests that the observed relaxation is predominantly from reorientation modes about axes perpendicular to the C—O bond, e.g. head-to-tail flips, comes from estimates of the electric dipole moment. Values of μ, from ϵ' versus 1/T (inset, Figure 1) and a simple Langevin–Debye model of orientation polarization [33], yield $\mu \sim 0.10$ D for a structure I clathrate of composition $CO{\cdot}5\frac{3}{4}\,H_2O$. Application of the Onsager equation [34], which considers additional polarization from reaction and cavity fields, affords $\mu \sim 0.13$ D. These dipole moment values are similar to those observed for carbon monoxide gas and α-solid [20, 27]. In order to account for the lower than expected intensity on the low temperature side of the absorption, a wide distribution of relaxation times about a mean value, τ, must be considered. Also, a larger relaxing component of the CO dipole in line with the applied field in the 12-hedron would increase the loss. In the calculation it is assumed that there are equal contributions of μ for CO reorientation in the small (S) and large (L) cages.

Other factors which tend to broaden the absorption are: (i) a temperature distribution across the sample, and (ii) the tail end of very low temperature absorptions such as from localized excitation modes often observed in amorphous and semi-crystalline materials [35]. Furthermore, the high temperature dielectric absorption, from the dipolar relaxation of the host water lattice (Figure 1), accounts for the extra loss on the high temperature side of the guest absorption.

At 10^7 Hz the experimental dielectric loss factor as a function of reciprocal temperature can be described by the equation;

$$\epsilon'' = \frac{\Delta\epsilon_S \cos(\alpha_S\pi/2)}{2\{\cosh((1-\alpha_S)\ln\omega\tau_S) + \sin(\alpha_S\pi/2)\}} + \frac{\Delta\epsilon_L \cos(\alpha_L\pi/2)}{2\{\cosh((1-\alpha_L)\ln\omega\tau_L) + \sin(\alpha_L\pi/2)\}} \tag{6}$$

for a symmetrical distribution of discrete relaxation times; S and L refer to the small and large cages which, for these calculations, are considered to be completely occupied. The optimum values in the above equation are: $\Delta\epsilon_S = 0.052$, $\alpha_S = 0.45$, $\tau_{0S} = 2.11 \times 10^{-10}$ s, $E_{aS} = 0.18$ kJ mol^{-1}, $\Delta\epsilon_L = 0.154$, $\alpha_L = 0.59$, $\tau_{0L} = 7.10 \times 10^{-11}$ s and $E_{aL} = 0.09$ kJ mol^{-1}. Figure 3 shows the calculated dielectric absorption at 10^7 Hz resolved into two component absorptions arising from the relaxation of CO in the two types of cages.

3.2. ^{13}C NMR RESULTS

Spectra are shown in Figures 4–7. The magic angle spinning spectrum shown in Figure 4 (see also Figure 1 of Ref. [1]) shows only a single line, which is quite symmetric (see inset) at the isotropic shift position. This result, which implies identical chemical shifts for ^{13}CO in the small and large cages, is rather surprising in that $^{13}CH_4$ in the small cage of its structure I hydrate has its resonance situated 2.4 ppm downfield from that in the large cage [36]. Distinct shifts have also been observed for other magnetic nuclei for a number of guest species occupying different cages [17, 22]. Why CO hydrate should be different in this respect is not immedi-

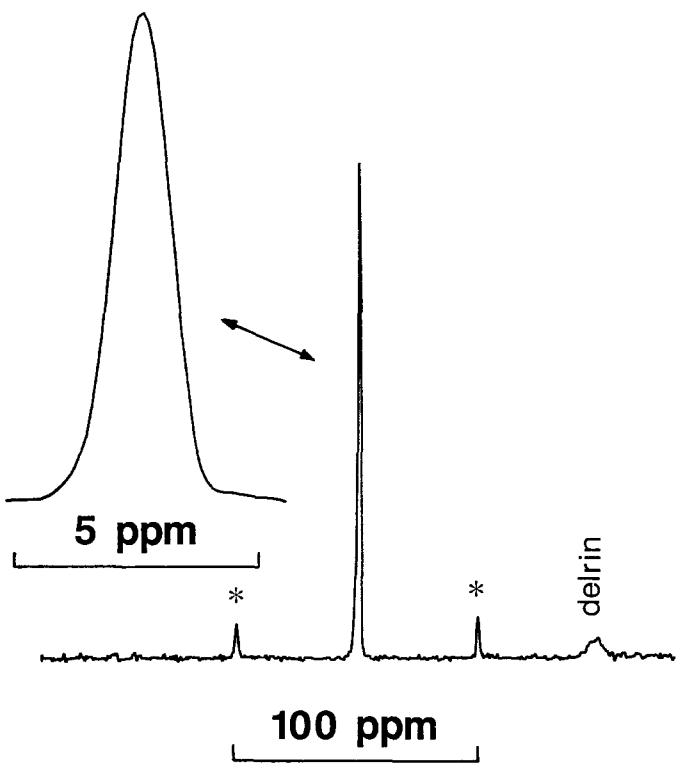

Fig. 4. CP/MAS ^{13}C NMR spectrum of ^{13}CO clathrate hydrate obtained at ~153 K. Spinning rate 2.2 kHz. Spinning side-bands are indicated by asterisks (*) and the signal from the delrin spinner is marked.

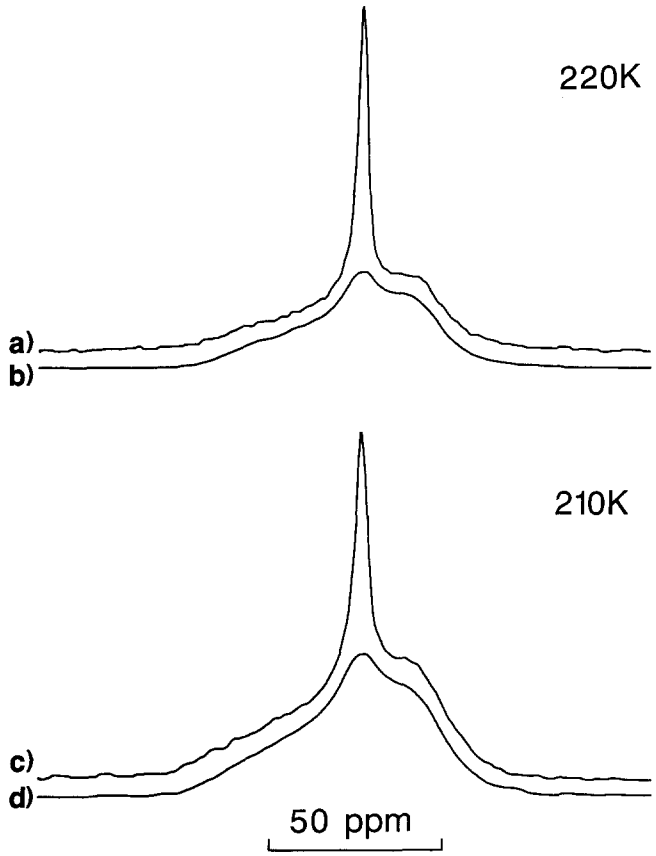

Fig. 5. Static ^{13}C NMR spectra of ^{13}CO clathrate hydrate at 210 and 220 K, with and without ^{1}H cross-polarization. (a), (c) Bloch decay spectra; (b), (d) CP spectra scaled for comparison with the Bloch decay spectra.

ately apparent, and as yet there is no model to describe the effect of the cage size on the shift observed for other species. (One might speculate, however, that the unusual behaviour of CO has to do with the fact that the C atom is involved in a triple bond and is already very much deshielded.)

The fact that the ^{13}CO can be detected by cross-polarization from ^{1}H to ^{13}C helps to establish that the sample is the hydrate of CO, since the technique relies upon the $^{1}H-^{13}C$ dipolar coupling, which would be averaged to zero by isotropic motion in the liquid or gas phases, and which would not be present in a physical mixture of ice and solid CO. (Although CO would not even be solid at the temperature studied.)

At the higher temperatures (>200 K) ^{13}CO, which was not present in the form of hydrate, was also detected in the simple Bloch decay experiments. These spectra (Figures 5a, c) show a much-increased intensity at the isotropic shift position when compared with the CP spectra (Figures 5b, d) at the same temperature. The increased intensity is presumably due to CO gas since the boiling point of liquid CO

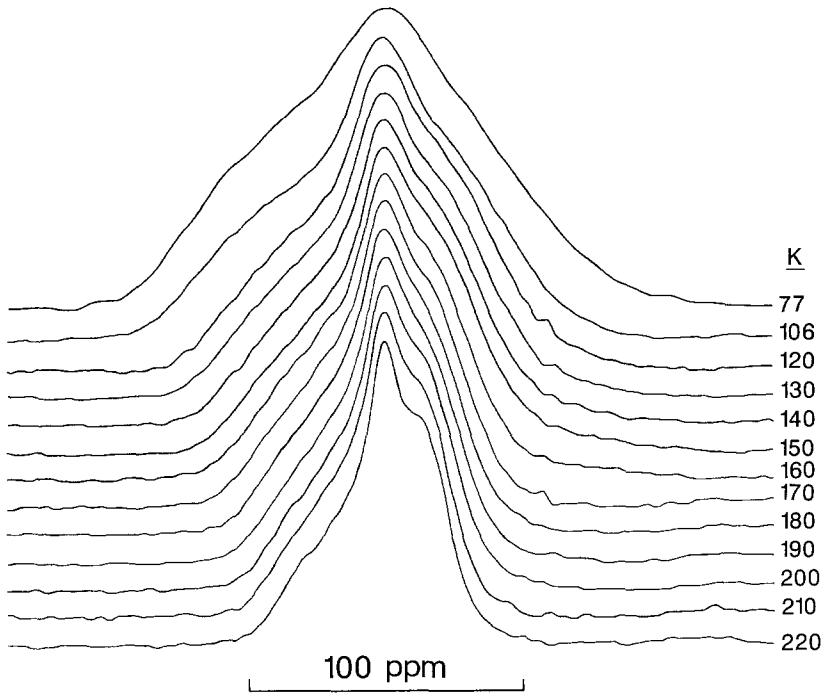

Fig. 6. Static CP ^{13}C NMR spectra of ^{13}CO clathrate hydrate from 77 to 220 K.

is 82 K. Note also the significant increase in the intensity of the gas component between 210 and 220 K which indicates increased dissociation of the hydrate.

Figure 6 shows the static CP spectra of ^{13}CO hydrate as a function of temperature. An important feature of the line shapes is that they show structure and anisotropy, even at 77 K. As the temperature increases the line shape narrows progressively and features become much clearer at the highest temperature, in much the same way as has been observed previously for other hydrates [15–17]. It has been found that in the range 200–270 K, depending on the nature of the guest, the water molecules of the cages begin to undergo rapid reorientation. The proton disorder, which is frozen-in at lower temperatures, is then averaged out and all the small or large cages effectively become identical. The line shape is no longer broadened on account of the distribution of slightly different cages which are present at lower temperatures. This situation has more or less been attained at 220 K in the CO hydrate.

The line shape at 220 K (Figure 6) very clearly shows an anisotropic axial ^{13}C tensor with an isotropic component superimposed. Since the CP spectra show only the solid material, these two components must correspond to ^{13}CO in the large (anisotropic) and small (isotropic) cages of structure I. Figure 7 shows a reasonably successful attempt to simulate the 220 K line shape: an anisotropic line shape, generated from well-known line shape functions [37], and a single frequency line at the isotropic position were added and then broadened with a Lorentzian function of 14.81 ppm half-width. A chemical shift anisotropy $\Delta\sigma = -56.97$ ppm and a ratio of

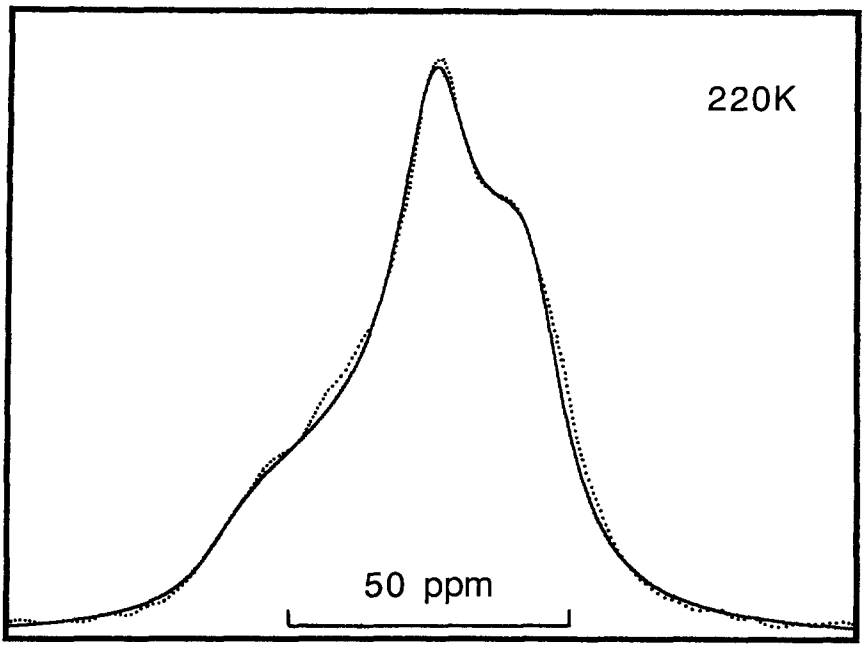

Fig. 7. Simulation of the static ^{13}C CP NMR spectrum of ^{13}CO clathrate hydrate at 220 K. Solid line = simulation; dotted line = experimental.

anisotropic : isotropic components of 1 : 0.37 were found to give the most reasonable agreement. In structure I hydrates there are three times as many large cages as small cages and thus the cage occupancy ratio $\theta_S/\theta_L = 1.11$ indicates slightly greater preference for the small cage, under the conditions prevalent in the sealed tube at 220 K.

We have previously attempted to rationalise the observed order parameter S (given as $\Delta\sigma_{ave}/\Delta\sigma_{static}$, the ratio of the averaged to static chemical shift anisotropies) for guests in the large cage of structure I in terms of motion of the guest. In the case of ^{13}CO a definite value of $\Delta\sigma_{static}$ is not yet known: the experimental results of Beeler *et al.* [38] on solid CO in the 15–20 K range gave $\Delta\sigma = 353$ ppm, but their *ab initio* calculations produced values in the 420–450 ppm range. The experimental results of Gibson *et al.* [39] at 4.2 K gave $\Delta\sigma = 365 \pm 20$ ppm. These authors judged that librational motion was still partially averaging the shift tensor and by attempting to take this motion into account they estimated $\Delta\sigma_{static} = 406 \pm 30$ ppm. A recent *ab initio* calculation using the 4–31 G basis set gave $\Delta\sigma = 427.48$ ppm [40]. Consequently we shall use a value $\Delta\sigma = 420$ ppm to calculate S and thus compare this with values for other structure I hydrates. The order parameter at 220 K is then $S = -0.136$. This places CO among the most mobile guest species so far observed in the structure I large cage, as might have been anticipated; only D_2S, D_2Se and CD_3F (for which $S = \pm 0.064$, ± 0.065 and ± 0.110 respectively [15–17]) have smaller order parameters. We can further emphasize this mobility by comparison with the results for the hydrate of CO_2, which is a much longer molecule. Regardless of the exact value of $\Delta\sigma_{static}$ for ^{13}CO it is clearly considerably larger than that for $^{13}CO_2$ ($\Delta\sigma = 334$ ppm) [16] and yet at

220 K the motionally averaged tensor for CO hydrate (-57 ppm) is significantly smaller than for CO_2 hydrate (-101 ppm). Similarly the line shape at 77 K shows that the CO molecule still has a great deal of orientational mobility, even though the line is now broadened by the distribution of different cage configurations brought about by the freezing-in of proton disorder. On the other hand, the motion of CO_2 in its hydrate at 77 K is much more constricted (see Figure 2 of Ref. [16]) and the line width is approaching that of a static CO_2 molecule. Previously we calculated the effects of Gaussian distributions in the value of $\Delta\sigma$ to simulate the effects of the distribution of cages at low temperature; see Figure 5 of Ref. [16]. At 77 K the CO_2 line shape corresponds most closely to a distribution with a half-width in $\Delta\sigma$ of about 0.8 of $\Delta\sigma_{\text{static}}$ centred at $\Delta\sigma_{\text{static}}$. Inspection of the same array of simulated line shapes suggests that CO hydrate at 77 K would be simulated reasonably well by a much narrower distribution with a half-width in $\Delta\sigma$ of about $0.2\,\Delta\sigma_{\text{static}}$ centred around $\Delta\sigma$ equal to about $-0.25\,\Delta\sigma_{\text{static}}$.

For CO_2 hydrate we presented one possible motional model for the high temperature regime, in which the CO_2 axis reorientates about the short (polar) axis of the large cage over a range of angles β out of the equatorial plane. The resulting expression for the averaged chemical shift anisotropy (Equation 5 of Ref. [16]) was

$$\Delta\sigma_{\text{ave}} = 0.5(1 - \cos\beta_{\max} - \cos^2\beta_{\max})\,\Delta\sigma_{\text{static}}.$$

If this model can be applied to CO hydrate then the value of $\beta_{\max}$ calculated using $S = -0.136$ is 43°, compared to 31° for CO_2. While the value for CO_2 seems reasonable, as discussed in [16], the angle for CO is surprisingly low: based on bond lengths for CO and CO_2 [41] and van der Waals radii in common use [42] their van der Waals lengths are 4.38 and 5.12 Å, respectively. This assumes that the van der Waals radius for the C of CO is the same as the half-thickness of an aromatic ring [42]. The radii from the cage centre to oxygen atoms of the cage have been given by Davidson [43] and, after subtracting the van der Waals radius of oxygen, the van der Waals radii of the large structure I cage range between 2.66 and 3.25 Å. Since the short axis of the cage passes through faces of the cage rather than the oxygens at the corners it is likely that the van der Waals cage diameter along this axis is a little less than the smallest radius to oxygen, i.e., less than $2 \times 2.66 = 5.32$ Å. CO_2 would have difficulty fitting along this short axis of the cage whereas CO would have no trouble at all. (Incidentally the van der Waals diameter of the small cage of structure I is 5.02 Å, which is a little too small for CO_2 but ample for CO).

It is worth investigating whether a different description might better explain the CO case, since the model discussed above, which seemed to be adequate for CO_2, is by no means unique. Description of the location and motion of molecules within a cage is at best tentative because there is not enough information available. One line of thought suggests that guest species might spend most of their time close to the walls of the cage rather than in the centre, possibly moving around very rapidly among several sites of marginally lower potential energy. (Experimental activation energies are generally very low for guest species as we have seen for CO hydrate from the dielectric results.) An alternative model may be developed based on the assumption that such sites exist at each face of the structure I large cage and that the CO molecule spends most of its time distributed among these sites, with its axis pointed roughly in the direction of the cage centre. There will then be two sites

(corresponding to the six-sided faces of the cage) where CO is oriented directly along the short cage axis and 12 sites (corresponding to the five-sided faces) where the CO is oriented at the angle β relative to the short axis of the cage.

The chemical shift of the ^{13}C nucleus is described by a second rank tensor σ, where the molecule is oriented along the z axis. The tensor components in a new coordinate frame where the short axis of the cage is along the z axis can then be determined from

$$\sigma' = R(\alpha, \beta, \gamma)\sigma R^{-1}(\alpha, \beta, \gamma)$$

where $R(\alpha, \beta, \gamma)$ are Euler angle rotation matrices [16, 44, 45]. Since the tensor for CO is also axial (by symmetry) γ can be set to zero.

In the case of very rapid reorientation among several sites j the resultant chemical shift tensor is given by the population weighted average of the chemical shift tensors σ_j' for each site:

$$\sigma'' = \frac{1}{n}\sum_{j=1}^{j=n} P_j \sigma_j'.$$

From the resulting tensor one can obtain the averaged chemical shift anisotropy and thus an expression for the order parameter S. Working through the mathematics with the assumption that all 14 sites have equal populations in the new model for CO hydrate then gives

$$S = \frac{9\cos^2\beta - 2}{7}$$

where, from the definition of the Euler angles, β is the angle between the short axis of the cage and the 12 CO positions which are off-axis. Substitution of the experimental value of S then gives $\beta = 70.0°$. (Note that an error of ± 30 ppm in the estimate of $\Delta\sigma_{\text{static}}$ for CO gives rise to an error of only $\pm 0.7°$ in the value of β.) This is remarkably close to the average angle between the short axis and the line joining the centre of the cage to the centre of a pentagonal face: 68.4°. If one adopts a similar model for CO_2 hydrate but with zero population of the 2 sites on the short axis of the cage the resulting expression is $S = (3\cos^2\beta - 1)/2$ from which $\beta = 68.7°$. The coincidence is again remarkable, though it is of no surprise that both molecules orientate with their axes close to the centre. It must be emphasized again, however, that the new model is no more unique than the previous one.

In conclusion, the dielectric studies have shown that CO is one of the fastest reorienting polar guests known in the clathrate hydrates, with an average $E_a = 0.14$ kJ mol^{-1}, giving rise to maxima in the dielectric loss factor in the low temperature range 2.2–3.8 K. The results can be interpreted in terms of distributions of relaxation times of guests in both the small and large cages, the distribution arising from the frozen-in disorder of the water molecule orientations. These conclusions are supported by the ^{13}C NMR results which show that CO occupies both cages, undergoing rapid reorientation even at 77 K.

Lineshapes with residual chemical shift anisotropy indicate anisotropic motion of CO in the large cage, and a feasible model has been presented for motion in the high temperature regime where the water reorientations are rapid. The cage occupancy ratio at 220 K, $\theta_S/\theta_L = 1.11$ shows that CO has a slightly greater preference for the

small cage, though the Langmuir constant for the large cage of structure I must still be large enough to ensure that this structure is formed rather than structure II which has a greater ratio of small to large cages. (Typical occupancy ratios for structure I hydrates of Xe and CH_4 are 0.73 and 0.916, respectively [4, 36].)

References

1. D. W. Davidson, M. A. Desando, S. R. Gough, Y. P. Handa, C. I. Ratcliffe, J. A. Ripmeester, and J. S. Tse: *Nature* **328**, 418 (1987).
2. D. W. Davidson, Y. P. Handa, C. I. Ratcliffe, J. S. Tse, and B. M. Powell: *Nature* **311**, 142 (1984).
3. J. S. Tse, Y. P. Handa, C. I. Ratcliffe, and B. M. Powell: *J. Incl. Phenom.* **4**, 235 (1986).
4. D. W. Davidson, Y. P. Handa, and J. A. Ripmeester; *J. Phys. Chem.* **90**, 6549 (1986).
5. D. W. Davidson, Y. P. Handa, C. I. Ratcliffe, J. A. Ripmeester, J. S. Tse, J. R. Dahn, F. Lee, and L. D. Calvert: *Mol. Cryst. Liq. Cryst.* **141**, 141 (1986).
6. A. Bar-Nun, G. Herman, D. Laufer, and M. L. Rappaport: *Icarus* **63**, 317 (1985).
7. G. J. Consolmagno: *J. Phys. Chem.* **87**, 4204 (1983).
8. J. Klinger: *J. Phys. Chem.* **87**, 4209 (1983).
9. A. H. Delsemme: *J. Phys. Chem.* **87**, 4214 (1983).
10. S. Wyckoff: *J. Phys. Chem.* **87**, 4234 (1983).
11. J. M. Greenberg, C.E.P.M. van de Bult, and L. J. Allamandola: *J. Phys. Chem.* **87**, 4243 (1983).
12. D. F. Strobel: *Intl. Rev. Phys. Chem.* **3**, 145 (1983).
13. S. L. Miller, in *Ices in the Solar System*, eds. J. Klinger, D. Benest, A. Dollfus, and R. Smoluchowski, Reidel, Dordrecht, 1985, p. 59.
14. J. I. Lunine and D. J. Stevenson: *Astrophys. J. Suppl. Ser.* **58**, 493 (1985).
15. D. W. Davidson, C. I. Ratcliffe, and J. A. Ripmeester: *J. Incl. Phenom.* **2**, 239 (1984).
16. C. I. Ratcliffe and J. A. Ripmeester: *J. Phys. Chem.* **90**, 1259 (1986).
17. M. J. Collins, D. W. Davidson, C. I. Ratcliffe, and J. A. Ripmeester: in *Dynamics of Molecular Crystals*, ed. J. Lascombe, Elsevier Science Publishers B.V., Amsterdam, 1987, p. 497.
18. S. R. Gough: *J. Phys. E. Sci. Instrum.* **15**, 530 (1982).
19. A. Pines, M. C. Gibby, and J. S. Waugh: *J. Chem. Phys.* **59**, 569 (1973).
20. A. L. McClellan: *Tables of Experimental Dipole Moments*, vol. 2, Rahara Enterprises, El Cerrito, California, 1974.
21. B. E. Read and G. Williams: *Trans. Faraday Soc.* **57**, 1979 (1961).
22. D. W. Davidson and J. A. Ripmeester: in *Inclusion Compounds*, eds. J. L. Atwood, J. E. D. Davies, and D. D. MacNicol, Academic Press, London, vol. 3, 1984, Ch. 3.
23. K. S. Cole and R. H. Cole: *J. Chem. Phys.* **9**, 314 (1949).
24. R. M. Fuoss and J. G. Kirkwood: *J. Am. Chem. Soc.* **63**, 385 (1941).
25. D. W. Davidson and R. H. Cole: *J. Chem. Phys.* **18**, 1417 (1951).
26. S. Liu and M. S. Conradi: *Solid State Commun.* **49**, 177 (1984).
27. K. R. Nary, P. L. Kuhns, and M. S. Conradi: *Phys. Rev. B* **26**, 3370 (1982).
28. N. R. Grey and L. A. K. Staveley: *Mol. Phys.* **7**, 83 (1983).
29. S. R. Gough, S. K. Garg, J. A. Ripmeester, and D. W. Davidson: *J. Phys. Chem.* **81**, 2158 (1977).
30. S. R. Gough, R. E. Hawkins, B. Morris, and D. W. Davidson: *J. Phys. Chem.* **77**, 2969 (1973).
31. A. Budó: *Physik Z.* **39**, 706 (1938).
32. K. Bergman, D. M. Roberti, and C. P. Smyth: *J. Phys. Chem.* **5**, 665 (1960).
33. J. H. Van Vleck: *The Theory of Electric and Magnetic Susceptibilities*, Oxford Press, New York, 1948.
34. L. Onsager: *J. Am. Chem. Soc.* **58**, 1486 (1936).
35. D. A. Ackerman, D. Moy, R. C. Potter, and A. C. Anderson: *Phys. Rev. B* **23**, 3886 (1981).
36. J. A. Ripmeester and C. I. Ratcliffe: *J. Phys. Chem.* **92**, 337 (1988).
37. M. Mehring: in *High Resolution NMR Spectroscopy in Solids, NMR Basic Principles and Progress*, Eds. P. Diehl, E. Fluck, and R. Kosfeld, Springer-Verlag, New York, 1976, vol. 2, p 21.
38. A. J. Beeler, A. M. Orendt, D. M. Grant, P. W. Cutts, J. Michl, K. W. Zilm, J. W. Downing, J. C. Facelli, M. S. Schindler, and W. Kutzelnigg: *J. Am. Chem. Soc.* **106**, 7672 (1984).
39. A. A. V. Gibson, T. A. Scott, and E. Fukushima: *J. Magn. Reson.* **27**, 29 (1977).

40. J. S. Tse: National Research Council Canada, personal communication.
41. *Tables of Interatomic Distances*, Chemical Society Special Publication No. 11, London, 1958, M117.
42. F. A. Cotton and G. Wilkinson: *Advanced Inorganic Chemistry*, 2nd Edition, Interscience, New York, 1966, p. 115.
43. D. W. Davidson: in *Water, a Comprehensive Treatise*, ed. F. Franks, Plenum, New York, 1973, vol. 2, p. 130.
44. R. J. Wittebort, E. T. Olejniczak, and R. G. Griffin: *J. Chem. Phys.* **84**, 5411 (1987).
45. C. I. Ratcliffe: *J. Phys. Chem.* **91**, 6464 (1987).
46. G. A. Jeffrey: in *Inclusion Compounds*, eds. J. L. Atwood, J. E. D. Davies, and D. D. MacNicol, Academic Press, London, Vol. 1, 1984, Ch. 5.